Mixing characterization inside microdroplets engineered on a microcoalescer

F. Sarrazin[a,*], L. Prat[a,*], N. Di Miceli[a], G. Cristobal[b], D.R. Link[c], D.A. Weitz[c]

[a] *Laboratoire de Génie Chimique (LGC), 5 rue Paulin Talabot, BP 1301, 31106 Toulouse, France*
[b] *RHODIA, Laboratoire du Futur (LOF), 178 avenue du Docteur Schweitzer, 33608 Pessac, France*
[c] *Physics Department, Harvard University, Oxford Street, Cambridge, MA, USA*

Abstract

We use a microdevice where microdroplets of reagents are generated and coalesce in a carrier continuous phase. The work focuses on the characterization of the mixing step inside the droplets, in the perspective to use them for chemical kinetic data acquisition. A dye and water are used, and an acid–base instantaneous chemical reaction is monitored thanks to a colored indicator. Acquisitions are done with a high-speed camera coupled to a microscope and a mixing parameter is calculated by image analysis. Different angles of bended channels and different ways of coalescence are compared. It is shown that the homogenization of the droplets can be reached in less than 10 ms after coalescence. This is achieved by forcing the droplets to coalesce in a "shifted" way, and later by adding 45° angle bends along the channel.
©

Keywords: Microreactor; Micro droplet; Mixing study; Fast reaction

1. Introduction

In the chemical industry and the fine chemistry, process fast design is a determining step for new molecule viability. To reduce the "time to market" industrial constraint, the product development phase can be reduced, contrary to toxicological tests, for example. The objective is to improve the initial steps of physical and chemical data acquisition, more particularly those allowing to determine chemical kinetic and transfer parameters. Then, that model knowledge is used to define the industrial process optimal operating conditions. Experimental strategy methodologies have already been developed and validated with success for kinetic parameters acquisition in classical batch reactors (Issanchou et al., 2003, 2005).

New microtools are developed for physical and chemical phenomena investigation, and more particularly for fast acquisition of chemical kinetic data and transfer parameters. They offer advantages for the fine chemical industry, more particularly the use of small amounts of products and the possibility to perform dangerous reactions.

One microchannel configuration to contact two reagents is the "coflow" reactor (Kamholz et al., 1999; Commenge et al., 2001; Baroud et al., 2003). Nevertheless, in that case, the coupling between diffusion and reaction has to be taken into account in order to analyze the experiments. Another possibility is to operate in a two-phase approach, where droplets are generated and transported in a continuous phase (Song and Ismagilov, 2003; Song et al., 2003a; Harries et al., 2003; Guillemet-Fritsch et al., 2004; Henkel et al., 2004). In this two-phase flow, heat and mass transfers are enhanced thanks to the high ratio existing between the interfacial surface and the volume of fluids. Moreover, droplets behave as batch reactors where the products mix and react. As they move at constant speed U along the channel, the distance d between the initial point and a given position in the channel corresponds to a reaction time $t = d/U$. Thus, this system is very convenient for kinetic data acquisition (Joanicot and Ajdari, 2005). The question is to determine the moment when the reagents are perfectly mixed within the droplet. Indeed, after this point, the variation of the droplet internal composition is only due to the chemical reaction, which is particularly interesting when the mixing time is negligible in

* Corresponding authors. Tel.: +33 5 56 46 47.
E-mail addresses: Flavie.Sarrazin@ensiacet.fr (F. Sarrazin), Laurent.Prat@ensiacet.fr (L. Prat

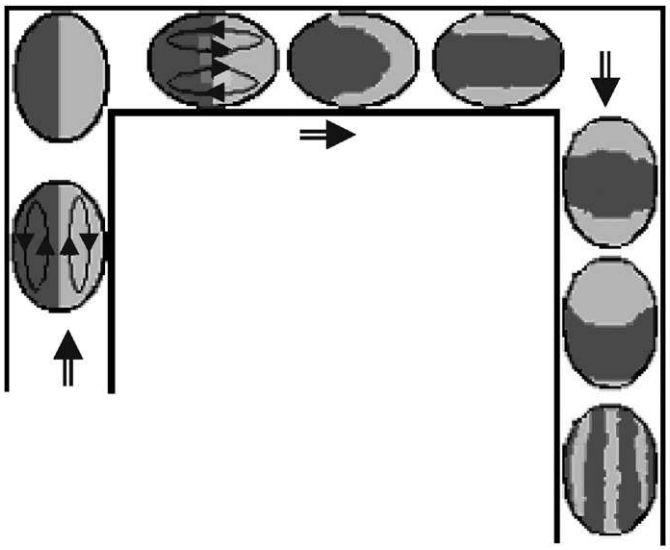

Fig. 1. Chaotic advection generated inside droplets flowing through a bent microchannel.

comparison with the reaction time. As the involved sizes are of several tens of micrometers, the droplet internal flows are laminar. A particular scenario corresponds to droplets that are large enough to be in contact with the four walls of the channel; in this case, forced convection phenomena install inside the circulating "slugs". In the reference frame of a droplet, periodic recirculation loops are formed symmetrically along the channel axis (Stone and Stone, 2005). This implies that there are no perpendicular convection streams to the main flow of the droplet. In the particular case where two chemical reagents are located within each hemisphere of a droplet, mixing mainly occurs by diffusion in the initial steps, and is later dominated by the forced advection. Such scenario is too slow and is not well adapted for fast kinetic acquisition purposes.

It has been shown that the mixing time is dramatically reduced by generating chaotic advection inside the droplets (Tice et al., 2003). This has been obtained by forcing to circulate nanoliter volume droplets in bent microchannels. At each bend, the internal loops are sheared and reoriented so that internal fluids mix (Fig. 1). This mixing process is commonly described by the "Baker transformation" (Song et al., 2003b): in the ideal case where the crossing of an angle reorients the circulation loops by 90°, the mixing time in a droplet is given by

$$t_{\text{theo}} = \frac{a.w}{U} \cdot \log(Pe), \tag{1}$$

where w is the channel width, a is the droplet length normalized by the channel width w, and Pe represents the Peclet number depending on the diffusion coefficient D:

$$Pe = \frac{w \cdot U}{D}. \tag{2}$$

In this work, we quantify different mixing scenarios. In order to generate two component droplets, we collapse two distinct drops in a controlled way. We compare the mixing properties of a fluidic device where mother droplets meet "side-by-side" with another fluidic device where the droplets merge in a shifted way, that is to say "one behind the other". Also, different bend angles varying between 45° and 135° are tested and compared. To do so, we use colored products inside the droplets and we monitor the mixing kinetics. This is obtained with a high-speed camera and the later image analysis gives us quantitative mixing parameter of isolated droplets. Finally, we perform colored acid/base reactions and contrary to the previous color dye experiments, droplets bleach as the fluids interpenetrate.

2. Materials and methods

2.1. Drop generation and coalescence

The device we use consists in generating pairs of droplets, each one containing a reactant, and in forcing them to coalesce (Fig. 2). The aqueous components A and B which form the droplets are injected in separate channels. Then, one-component droplets are naturally generated at the intersection of A or B with two oil streams, as it is usual in hydrophobic poly(dymethylsiloxane) (PDMS) channels (Thorsen et al., 2001). Two electrodes linked to a current generator are plugged inside the channel at the entrance of the solutions A and B. A 100 V voltage is applied between those electrodes, under a low-intensity current smaller than 1 mA. The result is that the mother droplets are polarized with opposite charges, which helps the synchronization and the coalescence (Link et al., 2006). In absence of current, droplets do not coalesce because the time of contact is too short to drain the film between them. After the coalescence, reactants A and B can mix and react inside monodisperse daughter droplets transported at constant velocity.

2.2. Device fabrication and dimensions

All the microchannel walls are made out of PDMS, which limits fluids wetting problems as all the walls are hydrophobic. On one part, a thin layer of PDMS is coated on a glass side. On another part, the channels are molted on a silica wafer designed thanks to SU8 soft lithography (Xia and Whitesides, 1998). Both parts are stuck on a flat part by contact after surface oxidation in a plasma chamber (Qin et al., 1996; Duffy et al., 1998; McDonald et al., 2000). The channel section is rectangular, with a constant height equal to 50 μm. The width varies between 30 and 100 μm depending on the position (droplet generation, meeting, or mixing); in the section where multi-component droplets circulate after the coalescence, the channel width is constant at 60 μm for all the studied geometries. The channel dimensions have been verified by profilometer measurements and electronic microscope observations. In all cases, the 50 μm height has been validated (deviation smaller than 3%) and the channel width precision has been estimated over 93%.

2.3. Operating conditions

The fluids are stocked in syringes placed on syringe pumps (Harvard Apparatus Ph2000) and they are flushed at constant

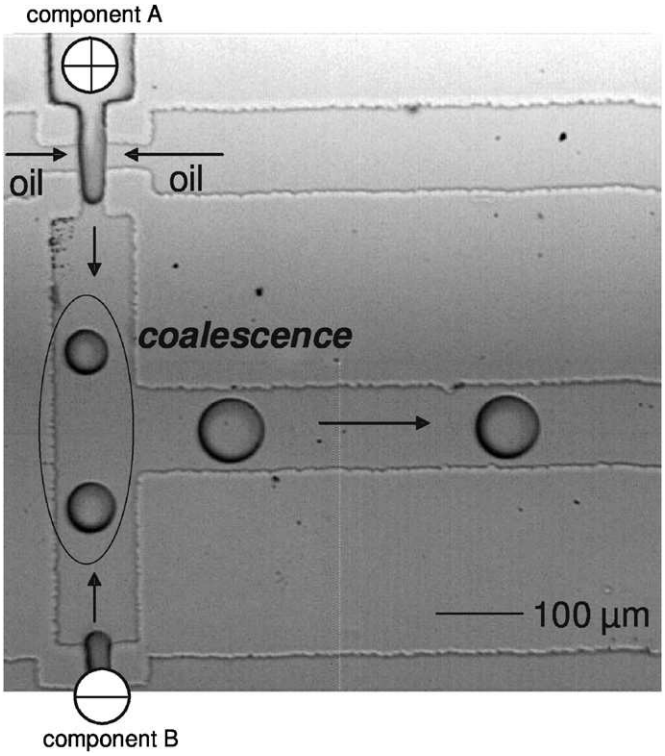

Fig. 2. Generation of multi-component droplets controlled by an electric field: opposite charged droplets are generated and transported in a continuous phase; they coalesce in the T-junction so that the resulting droplet can mix and react ("side-by-side" coalescence configuration).

flow rates into polyethylene tubing connected to the microchannels. Data acquisition is done thanks to a high-speed camera (Phantom V5 or APX Photron) coupled to a microscope operating with a $\times 10$ magnification objective (observation window surface $\sim 1\,\mathrm{mm}^2$). Image acquisition rate varies between 1000 and 5000 frames per second and the exposure time is about 50 µs.

The continuous phase is a silicone oil of viscosity $\mu = 0.02\,\mathrm{Pa\,s}$, density $\rho = 950\,\mathrm{kg/m}^3$ and interface tension with water $\sigma = 0.038\,\mathrm{N/m}$. As for the dispersed phase, two sets of products have been used for the mixing study. First, water and a dark dye (xylene cyanol) are injected at both extremities of the device. The contrast between them is clearly visible with the optical experimental setup (microscope and fast camera) in spite of the thin fluid layer observed. The molecular diffusion coefficient D is equal to $0.9 \times 10^{-9}\,\mathrm{m}^2/\mathrm{s}$, implying a time of about 2 s for the mixing of the two products by pure diffusion in a "coflowing" system for a channel width of 60 µm.

Second, acid and base are used and the reaction between them is followed by measuring the bleaching of a colored indicator. This is a protonic reaction:

$$\mathrm{A} + \mathrm{B} \xrightarrow{k} \mathrm{C} \tag{3}$$

with a kinetic constant $k \sim 10^8\,\mathrm{m}^3/\mathrm{mol\,s}$ and a neutralization time of about 10^{-8} s. So, it can be considered as instantaneous and the characteristic time is smaller than the mixing time. The chosen colored indicator is the $3', 3''$-dibromothymolsulfonphthalein sodium salt (i.e., bromothymol blue, called below BTB) whose color change takes place in the pH zone comprised between 6 and 7.6. The BTB solution is prepared by dissolving 1 mg of solid NaOH in a liter of water (final pH 8, color blue). The other reagent solution is made out of hydrochloric acid (pH 4, colorless). When those products meet in a 1:1 volume ratio conditions, the solution turns acidic (pH 4.3) and the BTB becomes yellow. Thus, in these conditions, the reaction can be assimilated to a "bleaching reaction" and its evolution can be monitored by using a standard gray-color high-speed camera.

3. Results and discussion

3.1. Flow data

Once the two reactant mother droplets coalesce under the controlled electric conditions, the resulting daughter droplets can be assimilated to 0.28 nL batch reactors generated at a frequency f of about 100 Hz. The dispersed phase flow rate is set constant and equal to 100 µL/h. The resultant microdroplets are monodisperse and present a slightly elongated shape with a height of 50 µm, a width of 60 µm, and a length of 110 µm. Their average velocity U is equal to 0.045/s and the corresponding particle Reynolds number is 0.18. On the other hand, the Peclet number corresponding to the forced convection induced by the channel walls is high and is equal to 3000 (Eq. (2)), which shows that within the droplets convective effects are much important than diffusive effects. As it is shown by Cristobal et al. (2006), this is a key factor to enhance the reagent mixing efficiency within the circulating droplets.

Fig. 3 shows the internal product behavior when mother drops perpendicularly coalesce and the resultant daughter droplets circulate in a straight channel. In this "side-by-side" coalescence device configuration, the inner droplet circulation loops present an axial symmetry. The reagents initially fill each of the droplet hemispheres. At the first mixing stages, they principally migrate from one hemisphere to the other by diffusion. The mixing kinetics is quite slow and mixing occurs within more than 70 ms. We have dramatically decreased the mixing time by arranging the two reagent hemispheres in the opposite orientation. This has been done by bending the channel (Fig. 5) or by changing the coalescence configuration of the mother droplets (Fig. 7). By doing this, we have overcome the first diffusion limiting step by taking advantage of the inner droplet convective effects.

3.2. Image analysis

As colored products and reactions are used to characterize the mixing within the circulating droplets, we have developed an adapted image analysis manipulation in order to determine a quantitative mixing parameter. This process is based on analyzing the homogeneity of the droplet gray-scale values within the drops.

To begin, the developed routines allow us to isolate and to label the droplets in order to follow them individually in time.

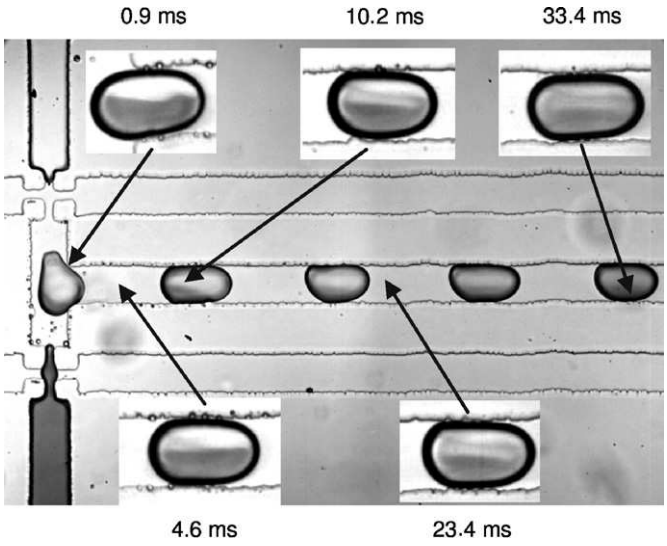

Fig. 3. Dye and water droplets flowing in a straight channel after "side-by-side" coalescence.

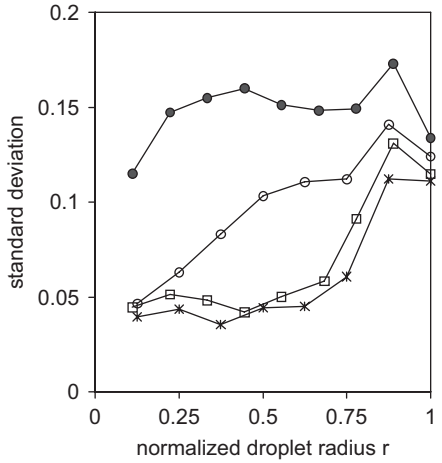

Fig. 4. Evolution of the standard deviation $\sigma_t(r)$ across the droplet concentric layers r at different mixing steps: * reference droplet (pure dye); □ well-mixed dye and water droplet; ○ partially mixed dye and water droplet; ● unmixed dye and water droplet.

The treatment is restricted to a sub-area of interest within the image related to the circulating droplets. To do so, we create a background mask containing the pixels whose intensity varies very little over all the frames of a movie. Then, a threshold is applied to the masked image; if the intensity range is properly chosen, this usually produces the outline of the droplets. Finally, a series of morphological procedures are applied and each droplet of the image is labeled. The procedure is applied for each individual image of the video. When this is done, a tracing algorithm keeps track of individual droplets by finding drops which partially overlap in successive images. The result is a sequence of isolated and labeled droplet.

The main point is to find a quantitative mixing parameter from the pixel gray-scale values. Preliminary tests have shown that the homogeneity of the background illumination in time is verified but the background illumination is not spatially constant along the channel. Furthermore, because of the droplet curved shape, even one-phase homogeneous droplets do not present a constant gray intensity on their interior. Then, neither the gray spectra mean value nor the standard deviation in the whole drop is a reliable criterion. To finish, the adequate method has been to cut the drops in concentric layers of one pixel width. In each layer, we have calculated an intensity standard deviation $\sigma_t(r)$ over a concentric layer r at a given mixing time t. Fig. 4 shows the evolution of the standard deviation σ_t versus r for a dye and water droplet at several mixing times t, and for a pure dye droplet. The r is the concentric layer index calculated from the external radius of the layer normalized by the total droplet radius, and is thus a dimensionless number comprised between 0 in the center of the drop and 1 on its interface. On the graph, it is possible to distinguish the mixing degrees of the dye and water droplet by comparing its standard deviation evolution with the results obtained for the one-component drop taken as a reference: the dye and water droplet value approaches the reference ones as it mixes.

Thus, it is possible to follow the mixing kinetics of a droplet by comparing its standard deviation at different stages with the reference values of an homogeneous droplet. This is particularly clear in the central region of the droplet, below the normalized radius $r_2 = 0.75$. Indeed, when r is superior to r_2, the layers correspond to the very dark pixels that represent the droplet interface, and do not reflect the mixing stages. Eventually, the mixing stage of a droplet at a given time t is represented by the dimensionless number χ calculated from

$$\chi(t) = \frac{\overline{\sigma}_t - \overline{\sigma}_{\text{ref}}}{\overline{\sigma}_0 - \overline{\sigma}_{\text{ref}}}. \tag{4}$$

In this expression, $\overline{\sigma}_t$ represents the mean over r of $\sigma_t(r)$ at a given time t:

$$\overline{\sigma}_t = \frac{1}{r_2} \cdot \int_0^{r_2} \sigma_t(r) \cdot \mathrm{d}r. \tag{5}$$

$\overline{\sigma}_{\text{ref}}$ corresponds to the mean over r of the standard deviation for the reference droplet (pure dye). The $\overline{\sigma}_0$ is the value obtained for the analyzed droplet at the initial time $t = 0$, just after the daughter droplet formation.

This method overcomes the unwanted effects due to the light spatial non-homogeneity and the droplet shape. When χ values are definitively below 5%, the droplet can be considered as perfectly mixed. Furthermore, it has been checked that the evolution of the mixing parameter is reproducible and similar for several droplets at a given time.

3.3. Comparison between straight and bent channels

We have quantified the mixing efficiency of bent channels containing different angles located immediately after the perpendicular "side-by-side" coalescence. As previously discussed, the angles induce different orientations inside the drops when they flow through the winding channels. We have used the above-described mixing parameter in order to compare the

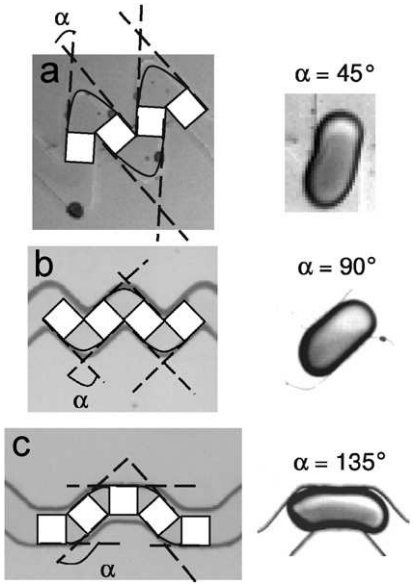

Fig. 5. The 45°, 90°, and 135° bending channels.

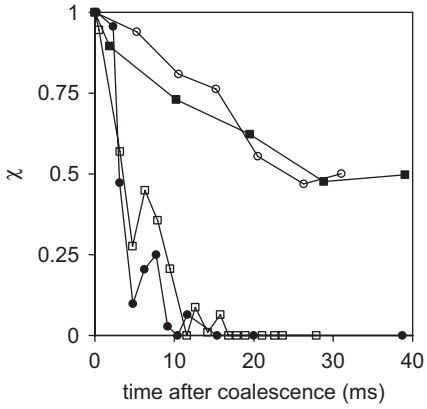

Fig. 6. Mixing parameter evolution versus time for dye and water droplets flowing through bent channels of different angle degrees after the "side-by-side" coalescence configuration: • $\alpha = 45°$ (channel a); □ $\alpha = 90°$ (channel b); ○ $\alpha = 135°$ (channel c); ■ straight channel.

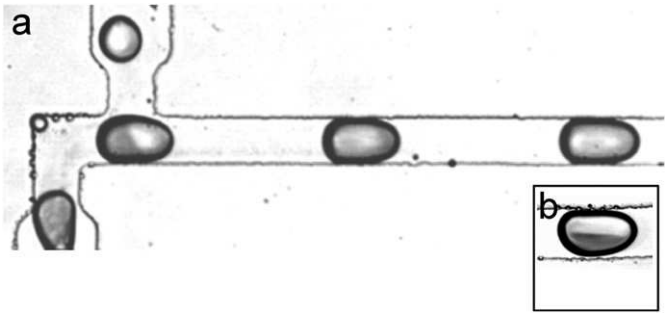

Fig. 7. Dye and water droplets generated by the "shifted" coalescence and transported in a straight channel. The pictures on the right show the droplet 6 ms after the different kinds of coalescence: (a) shifted coalescence; (b) "side-by-side" coalescence.

different mixing scenarios. Three devices containing angles of different values (α) have been studied: 135°, 90°, and 45°. The channel length between two successive angle curves has been set equal to the width of the channel w. By doing this, between two rotations, the droplets circulate by a distance equivalent to their length so that a complete recirculation loop can take place within them. This condition is not perfectly met for the 135° angle channel, which will be discussed below. For each scenario, Fig. 5 illustrates the channel design, the geometrical construction and a snapshot of a typical droplet after two reorientations.

All the droplets are formed at the same conditions and reach the entrance of the bending channel within less than 1 ms after coalescence. At this position which corresponds to the initial mixing time, all the analyzed droplets have the same "Janus"-like fluid orientation. They are separated into two hemispheres containing the dye and the water, as previously shown in Fig. 3. The evolution of the mixing parameter (Eq. (4)) inside the two-component droplets after coalescence is illustrated in Fig. 6 for different angles α and is compared to the simple straight channel case.

Two dramatically different trends can be highlighted here. Whereas the 45° and 90° bend configurations show a very efficient mixing property, the 135° one appears to offer a mixing efficiency closer to the straight channel. As for this latter simple case, the 135° bent channel does not sufficiently shear the droplets. Thus, it cannot force the inner fluid reorientation and the mixing time is about 70 ms.

Besides, smaller angle bends (channels a and b) seem to be much more efficient for contacting the droplet inner fluids. They offer reduced mixing times of about 10 ms at the previously described experimental conditions. In those two angle scenarios, the mixing parameter strongly decreases in the first milliseconds as the droplets cross the first angle. It then starts oscillating before it reaches the value of zero. These oscillations are very probably due to three-dimensional flow effects within the droplets. Indeed, layers of fluids are formed and reoriented inside the drops, which is seen by the camera as alternating dark and clear gray-color levels. In both cases, the droplets appear to be completely mixed after flowing through three bends. Moreover, the results obtained here tend to approach to the ideal value of 8.5 ms calculated from the "Baker transformation" theory (Eq. (1)) at the same experimental flow conditions.

3.4. Comparison of the two coalescence configurations

In order to faster the mixing kinetic times without adding any bending angle to the reactant droplet path, we have explored a new way of combining droplets where we force the two reactant drops to coalesce in a "shifted" way (Fig. 7). The two upstream mother droplet producing channels are no longer aligned in a T-junction but slightly shifted one respect to the other. The resulting droplet coalescence is not "side-by-side" as before, but can more accurately be described as "one after the other". In such a configuration, the two reactant "interface" inside the daughter droplets is perpendicular to the main stream line and no longer aligned with the channel axis. At once, the

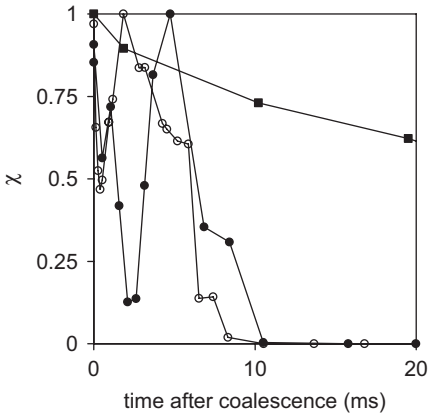

Fig. 8. Mixing criterion evolution versus time inside droplets flowing through straight channels for different coalescence and product systems: ■ dye and water after a "side-by-side" coalescence configuration; • dye and water after a "shifted" coalescence configuration; ○ bleaching reaction after a "shifted" coalescence configuration.

forced natural convection inside the droplets helps the inner homogenization and mixing is dramatically accelerated. This mechanism has been theoretically described by Handique and Burns (2001).

We have studied the influence of the coalescence geometry over the mixing kinetics in a straight channel. To do so, we have first monitored the homogenization kinetics of a dye contained in one of the hemispheres of a droplet, and later followed the bleaching kinetics of the reaction described in Section 2.3. The results obtained with both systems are identical (Fig. 8): in the "shifted coalescence" configuration, the complete droplet mixing, which is emphasized by the zero value of the mixing parameter, is achieved in around 10 ms, whereas only partial mixing is observed at 40 ms in the "side-by-side" coalescence configuration. As in the previous paragraph, the mixing parameter significantly oscillates in the first milliseconds after the coalescence. This might be explained by the need for several internal circulation loops in order to homogenize the droplets. Thus, the mixing parameter oscillations are probably due to the tridimensional "back and forth" circulation of the unmixed dye sheets. Besides, the "bleaching reaction" experiments confirm that poorly circulating "dead" zones appear inside the droplets. These zones might also have some influence in the mixing parameter oscillations.

In fact, as the bleaching reaction is instantaneous, it is possible to underline the zones where the mixing slowly occurs (see Section 2.3). By inversing the initial configuration of the two reagents, those zones can be investigated successively on the rear and on the front of the droplets. In both cases, stagnant regions are pointed out. In order to illustrate this, different images of reactive droplets have been taken 4 ms after the meeting of the reagents. These two snapshots are shown in Fig. 9 for both initial conditions. It seems that different zones inside the droplets are not well mixed at this point and some easily distinguishable regions at the back or front of the droplet still remain dark. This can be only explained by the presence of non-circulating or static points within the drops. This might

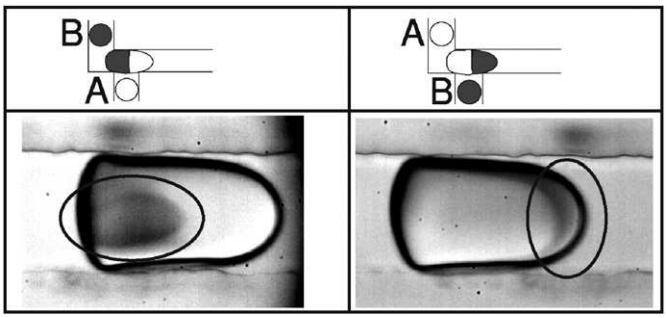

Fig. 9. Acid–base reaction followed by a colored indicator: detail of the droplet 4 ms after the coalescence for two initial configurations of the reagents (reagent A = HCl; reagent B = BTB and NaOH).

underline that the main convection loops do not reach those "dead" regions. As a result, the acid can only migrate into them by diffusion. This is probably the reason why the mixing is totally achieved within 10 ms in such coalescence geometry, and not before.

To finish it is possible to compare the mixing efficiency between the "shifted coalescence" and the winding channels. It appears that the mixing time obtained with the best angle bend scenario is comparable to the "shifted coalescence" case. One might think that by combining both strategies we will be able to homogenize a microdroplet containing two reactants faster than 10 ms.

4. Conclusion

This work is based on the use of high-speed camera movie acquisition and on a later image analysis in order to quantify the mixing step within multi-component droplets circulating through microfluidic devices. A spatial mixing parameter has been defined and applied inside each droplet. The main advantage of the device under test is to easily control the coalescence of reagent droplets and to improve the mixing within them. As the droplets touch the walls of the channels, the forced convection generated in the plugs helps the homogenization by convection. The present study leads to the design of an ideal mixing microreactor by combining the "shifted" coalescence and 45° bended channels.

In the improved device, the mixing time is smaller than 10 ms. Thus, after this time, droplets can be considered as perfectly homogeneous for the kinetic parameter acquisition of a chemical reaction taking place within the droplets. Nevertheless, the presence of dead zones has been observed at the back and front of the droplets. Thus, it seems important to characterize in more detail the hydrodynamics of droplet transport in microchannels. Further simulations and microparticle image velocimetry experiments are in perspective so as to characterize the velocity field, and check the presence of different structures inside the drops.

Acknowledgments

We sincerely acknowledge G. Casamatta and C. Gourdon from the Laboratoire de Génie Chimique and M. Joanicot from

RHODIA-CNRS Laboratoire du Futur for supporting this study. We also acknowledge R. Koetitz for his participation in image analysis.

References

Baroud, C.N., Ménétrier, L., Okkels, F., Tabeling, P., 2003. Measurement of fast kinetics in a microfluidic system. In: Seventh International Conference on Micro TAS, California, USA.

Commenge, J.M., Falk, L., Corriou, J.-P., Matlosz, M., 2001. Microchannel reactors for kinetics measurement: influence of diffusion and dispersion on experimental accuracy. Récents Progrès en Génie des Procédés 15 (80),

Cristobal, G., ArbouetArbouet, L., Sarrazin, F., Talaga, D., Bruneel, J.-L., Joanicot, M., ServantServant, L., 2006. On-line laser Raman spectroscopic probing of droplets engineered in microfluidic devices. Lab Chip 6, 1140–1146.

Duffy, D.C., McDonald, J.C., Schueller, O.J.A., Whitesides, G.M., 1998. Rapid prototyping of microfluidic systems in poly(dimethylsiloxane). Analytical Chemistry 70, 4974–4984.

Guillemet-Fritsch, S., Aoun-Habbache, M., Sarrias, J., Rousset, A., Jongen, N., Donnet, M., Bowen, P., Lemaître, J., 2004. High-quality nickel manganese oxalate powders synthesized in a new segmented flow tubular reactor. Solid State Ionics 171, 135–140.

Handique, K., Burns, M.A., 2001. Mathematical modeling of drop mixing in a slit type microchannel. Journal of Micromechanics and Microengineering 11, 548–554.

Harries, N., Burns, J.R., Barrow, D.A., Ramshaw, C., 2003. A numerical model for segmented flow in a microreactor. International Journal of Heat and Mass Transfer 46, 3313–3322.

Henkel, T., Bermig, T., Kielpinski, M., Grodrian, A., Metze, J., Kölher, J.M., 2004. Chip modules for generation and manipulation of fluid segments for micro serial flow processes. Chemical Engineering Journal 101, 439–445.

Issanchou, S., Cognet, P., Cabassud, M., 2003. Precise parameter estimation for chemical batch reactions in heterogeneous medium. Chemical Engineering Science 58, 1805–1813.

Issanchou, S., Cognet, P., Cabassud, M., 2005. Sequential experimental design strategy for rapid kinetic modelling of chemical synthesis. A.I.Ch.E. Journal 51, 1773–1781.

Joanicot, M., Ajdari, A., 2005. Droplet control for microfluidics. Science 309, 887–888.

Kamholz, A.E., Weigl, B.H., Finlayson, B.A., Yager, P., 1999. Quantitative analysis of molecular interaction in a microfluidic channel. Analytical Chemistry 71, 5340–5347.

Link, D.R., Grasland-Mongrain, E., Duri, A., Sarrazin, F., Cheng, Z., Cristobal, G., Marquez, Weitz, D.A., 2006. Electric control of droplets in microfluidic devices. Angewandte Chemie, International Edition 45 (16), 2556–2560.

McDonald, J.C., Duffy, D.C., Anderson, J.R., Chiu, D.T., Wu, H., Schueller, O.J.A., Whitesides, G.M., 2000. Fabrication of microfluidic systems in poly(dimethylsiloxane). Electrophoresis 21, 27–40.

Qin, D., Xia, Y., Whitesides, G.M., 1996. Rapid prototyping of complex structures with feature sizes larger than 20 µm. Advanced Materials 8, 917–921.

Song, H., Ismagilov, R.F., 2003. Milliseconds kinetics on a microfluidic chip using nanoliters of reagents. Journal of the American Chemical Society 125, 14613–14619.

Song, H., Tice, J.D., Ismagilov, R.F., 2003a. A microfluidic system for controlling reaction network in time. Angewandte Chemie, International Edition 42(7).

Song, H., Bringer, M.R., Tice, J.D., Gerdts, C.J., Ismagilov, R.F., 2003b. Experimental test of scaling of mixing by chaotic advection in droplets moving through microfluidic channels. Applied Physics Letters 83(22).

Stone, Z.B., Stone, H.A., 2005. Imaging and quantifying mixing in model droplet in a micromixer. Physics of Fluids 17, 063103.

Thorsen, T., Roberts, F.H., Arnold, F.H., Quake, S.R., 2001. Dynamic pattern formation in a vesicle-generating microfluidic device. Physical Review Letters 86, 4163–4166.

Tice, J.D., Song, H., Lyon, A.D., Ismagilov, R.F., 2003. Formation of droplets and mixing in multiphase microfluidics at low values of the Reynolds and the capillary numbers. Langmuir 19, 9127–9133.

Xia, Y., Whitesides, G.M., 1998. Soft lithography. Angewandte Chemie, International Edition 37, 550–575.